10 μm minority-carrier diffusion lengths in Si wires synthesized by Cu-catalyzed vapor-liquid-solid growth

Morgan C. Putnam,[a] Daniel B. Turner-Evans, Michael D. Kelzenberg, Shannon W. Boettcher, Nathan S. Lewis, and Harry A. Atwater
California Institute of Technology, 1200 E. California Blvd., Pasadena, California 91125, USA

(Received 5 August 2009; accepted 18 September 2009; published online 23 October 2009)

The effective electron minority-carrier diffusion length, $L_{n,\mathrm{eff}}$, for 2.0 μm diameter Si wires that were synthesized by Cu-catalyzed vapor-liquid-solid growth was measured by scanning photocurrent microscopy. In dark, ambient conditions, $L_{n,\mathrm{eff}}$ was limited by surface recombination to a value of ≤ 0.7 μm. However, a value of $L_{n,\mathrm{eff}}=10.5\pm1$ μm was measured under broad-area illumination in low-level injection. The relatively long minority-carrier diffusion length observed under illumination is consistent with an increased surface passivation resulting from filling of the surface states of the Si wires by photogenerated carriers. These relatively large $L_{n,\mathrm{eff}}$ values have important implications for the design of high-efficiency, radial-junction photovoltaic cells from arrays of Si wires synthesized by metal-catalyzed growth processes. © *2009 American Institute of Physics*. [doi:10.1063/1.3247969]

Photovoltaic cells based on Si wire arrays offer a number of features that are compatible with obtaining high device performance through the use of low-cost fabrication steps. Some of these features include the opportunity to optimize carrier collection through formation of either radial or axial *p-n* junctions, the ability to directly synthesize large-area arrays of Si wires through the use of chlorosilane precursors, and the ability to embed the resulting Si wire arrays in flexible polymeric sheets; thus enabling the facile removal of the Si wire arrays and concomitant reuse of the templating growth substrate.[1–4]

The vapor-liquid-solid (VLS) growth mechanism provides a demonstrated pathway to the fabrication of arrays of one-dimensional Si wires.[1] However, VLS growth processes that employ metallic precursors unavoidably result in metal incorporation into the Si wires. The presence of metallic impurities has the potential to degrade the minority-carrier lifetime and diffusion length in the Si wires. Hence, measurements of the minority-carrier diffusion length are critical for assessing the potential of VLS-grown Si wire arrays as components in the fabrication of efficient photovoltaics.

Minority-carrier diffusion lengths up to 4 μm have been reported for Au-catalyzed, VLS-grown Si wires.[3,5] These values are considerably smaller than the diffusion length in high-purity bulk Si, but are in good agreement with the value expected based on the measured concentration of the known deep trap, Au, in the Si wires.[6] Cu-catalyzed, VLS-grown Si wires are expected to have longer diffusion lengths than wires grown from Au catalysts, because Cu is not as detrimental as Au to the minority-carrier lifetime of Si.[7,8] We report herein, through use of scanning photocurrent microscopy (SPCM), an effective electron minority-carrier diffusion length, $L_{n,\mathrm{eff}}$, of 10.5 ± 1 μm for Cu-catalyzed VLS-grown Si wires.

Cu-catalyzed Si wires were grown at 1000 °C and 1 atm from a 500:10 standard cubic centimeters per minute (SCCM) gaseous H_2:$SiCl_4$ stream, in a process similar to that reported previously[1] (see supporting information[9]). The as-grown undoped wires were 2.0 μm in diameter and $\sim$100 μm in length. These wires were highly resistive, so in subsequent growths 0.06 SCCM BCl_3 (5% in H_2) was added to the reactant stream. Four-point probe measurements of wires that were removed from the Si growth substrate indicated that the wires were *p*-type with a resistivity of 0.19 ± 0.02 Ω cm. This value corresponds to an acceptor concentration N_A of $(1.05\pm0.15)\times10^{17}$ cm^{-3}, assuming a bulk hole mobility (3.1×10^2 cm^2 V^{-1} s^{-1}) for Si. Prior to SPCM characterization, a 5:1:1 (by volume) mixture of de-ionized H_2O (18 MΩ cm resistivity):NH_4OH(29%):H_2O_2(30%) (RCA1) was used to remove any organic contamination, and a 6:1:1 (by volume) mixture of de-ionized H_2O:HCl(37%):H_2O_2 (RCA2) was used to remove residual Cu. The chemical/native oxide was then removed by etching the wires for 15 s in buffer HF Improved (Transene, Inc.). The wires were then exposed to air for 3.5 days to grow a native oxide on the wires.

To obtain diffusion lengths from the SPCM method, both an Ohmic and a rectifying contact were required on the Si wires.[3,5] The Si wires were first removed from the growth substrate and dispersed onto a Si_3N_4-coated Si(100) wafer. Photolithography was then used to pattern the contacts onto individual Si wires. Following a 15 s etch in Buffer HF Improved to remove the native oxide, Ohmic contacts were formed by sputtering Al (with 1% Si) onto the *p*-Si wires. Rectifying contacts were then formed by sputtering Al onto the native oxide of the *p*-Si wires. This metal-insulator-semiconductor (MIS) contact between Al and *p*-Si produces a rectifying contact.[10] After deposition of metal, a contact anneal was performed at 300 °C for 10 min in forming gas (5% H_2 in N_2).

Figure 1 illustrates the observed rectifying behavior for a device with an ideality factor of 1.8 and an effective barrier height of 0.6 eV. Ideality factors ranged from 1.4 to 3.1, and the effective barrier height ranged from 0.4 to 0.7 eV. The inset of Fig. 1 displays an optical microscope image of the device. The bright spot near the center of the wire corre-

[a]Electronic mail: putnam@caltech.edu.

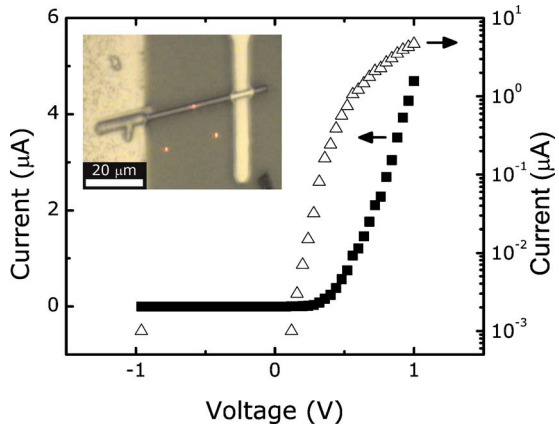

FIG. 1. (Color online) Current-voltage sweep of a 2.0 μm diameter Si wire device. Inset: optical microscope image of the measured device; the Ohmic contact is on the left and the MIS contact is on the right. The laser illumination spot can be seen in the center of the wire.

sponds to the area illuminated by the laser, while the other two spots are artifacts that arose from reflections in the microscope optics.

SPCM measurements were made using a WiTec scanning near-field optical microscope in confocal mode. Local illumination was provided by a 650 nm laser, chopped at 30 Hz, with a diffraction limited spot size of 0.4 μm. Broad-area illumination was provided by the microscope light (color temperature=3200 K). Using a photodiode to measure the illumination power density, the optical carrier generation density for both sources was calculated to be a factor of 40 less than the equilibrium hole concentration of 1×10^{17} cm^{-3}, thus satisfying the requirement for low-level-injection illumination conditions (see supporting information). The photocurrent from the MIS rectifying contact was detected by a preamplifier connected to a lock-in amplifier.[3] For measurements at an applied bias, the Ohmic contact was connected to a dc voltage source.

In SCPM, a two-dimensional map of the photocurrent is generated by recording the photocurrent while scanning the sample underneath a local illumination source (the 650 nm laser). Figure 2 depicts the zero-bias SPCM images of a Cu-catalyzed Si wire measured in the dark [Fig. 2(b)] and in the presence of broad-area illumination [Fig. 2(c)]. In the dark, a small photocurrent (note respective scale bars) was observed along the wire, as well as on the MIS rectifying contact in regions immediately above and below the wire. The photocurrent above and below the wire on the MIS contact is believed to arise from an optically thin coating of Al that formed, as a result of the directional nature of sputtering and the large ratio of the wire diameter to the thickness of the contact, along the sidewall of the wire. Under broad-area illumination, a much larger signal, which extended greater than half the length of the device, was observed. Figure 2(a) depicts a scanning electron microscope (SEM) image to facilitate correlation of the observed photocurrent response with the geometry of the device.

The larger amplitude of the photocurrent and the increased distance over which photocurrent was observed are indicative of a larger effective electron minority-carrier diffusion length, $L_{n,\mathrm{eff}}$, under broad-area illumination than in the dark. Because of the observed long time decay in $L_{n,\mathrm{eff}}$ (time scale of minutes) after removal of the broad-area illumination, as shown by the dark photocurrent response after exposure to broad-area illumination [Fig. 2(d), Fig. S1[9]], we assume that an improvement in surface passivation produces the increase in $L_{n,\mathrm{eff}}$ with broad-area illumination. An increase in $L_{n,\mathrm{eff}}$, as a result of an increase in the bulk lifetime, would be expected to decay on the time scale of the minority-carrier lifetime (10–100 ns).

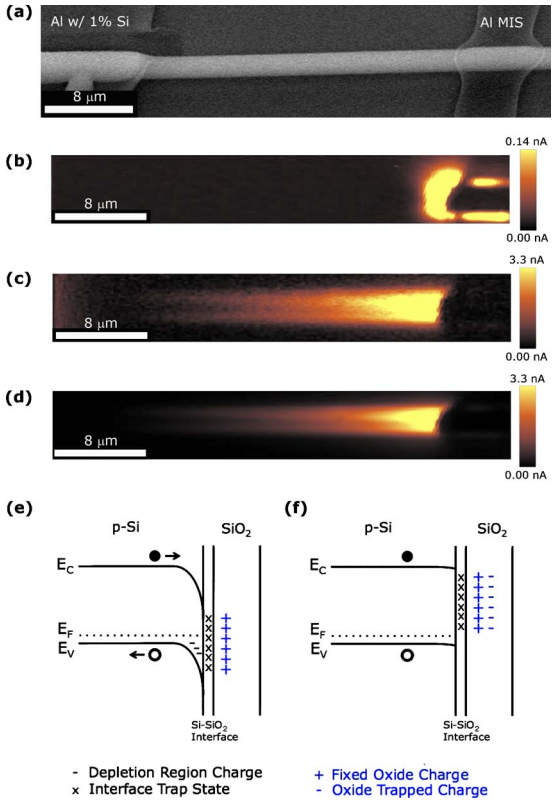

FIG. 2. (Color online) (a) SEM image of the device of Fig. 1. (b) SPCM image of the device measured in the dark. (c) SPCM image of the device measured under low-level-injection, broad-area illumination. (d) SPCM image of the device measured in the dark for a measurement started within 5 s after exposure to broad-area illumination. All SPCM images are at zero bias and took 4 min and 14 s to acquire. (e) Schematic illustration of the proposed band diagram in the dark. (f) Schematic diagram of the proposed band diagram under broad-area illumination.

The photoinjection of electrons into the oxide (oxide trapped charge)[11] could produce a decrease in the surface recombination velocity S and is consistent with the long time decay in $L_{n,\mathrm{eff}}$. Figure 2(e) depicts the expected band structure for p-Si coated with a native oxide that contains positive fixed oxide charge. The presence of positive fixed oxide charge, which is well known to exist in SiO_2,[12,13] will introduce negative surface band bending. This band bending will result in a large minority-carrier surface concentration and hence produce a high surface-recombination velocity. However, the photoinjection of electrons into the oxide could balance the positive fixed oxide charge, thereby reducing the negative surface band bending and decreasing S [Fig. 2(f)]. A long time scale (time scale of minutes) for electrons to tunnel out of an oxide[14] is consistent with the observed long time decay in $L_{n,\mathrm{eff}}$ under the proposed surface passivation mechanism.

Figure 3 displays photocurrent cross sections along the length of the wire, taken from SPCM images, as a function of the bias voltage applied to the Ohmic contact. These data allowed calculation of values of $L_{n,\mathrm{eff}}$ based upon the ex-

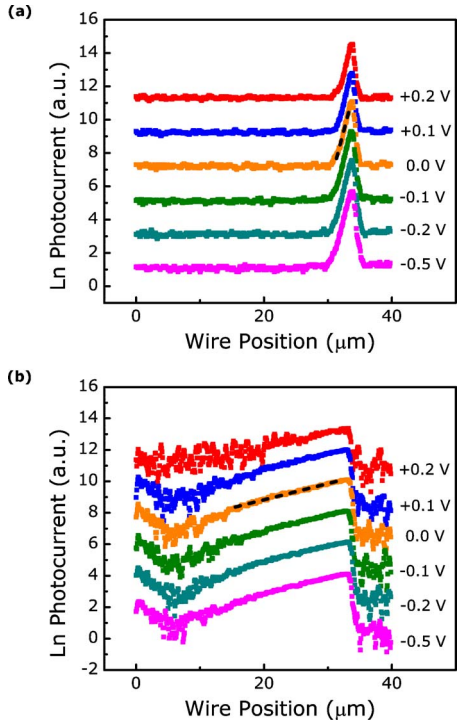

FIG. 3. (Color online) Photocurrent cross sections along the length of the wire, as a function of the bias voltage applied to the Ohmic contact. (a) Measured in the dark (b) and measured under low-level-injection, broad-area illumination. In both [(a) and (b)] the zero-bias fit is shown as a dashed black line and is used to calculate effective electron minority-carrier diffusion lengths $L_{n,\mathrm{eff}}$ of <0.7 and 9.7 μm, respectively.

pected relationship for diffusion-limited minority-carrier transport in the quasineutral region: $J_{\mathrm{ph}} \propto \exp[-(x_{\mathrm{MIS}}-x)/L_{n,\mathrm{eff}}]$, where $x_{\mathrm{MIS}}-x$ is the distance between the MIS rectifying contact and the laser illumination. Under broad-area illumination, the best-performing individual device exhibited a value of $L_{n,\mathrm{eff}}=9.5\pm0.2$ μm for photocurrent cross sections along the center of the wire and a value of $L_{n,\mathrm{eff}}=11.5\pm0.2$ μm for photocurrent cross sections along the sidewall of the wire [Fig. 2(c): see supporting information], producing an average $L_{n,\mathrm{eff}}$ of 10.5 ± 1 μm for this sample. Measurements in the dark yielded $L_{n,\mathrm{eff}}\leq0.7$ μm. The value of $L_{n,\mathrm{eff}}$ measured in the dark is an upper bound for the actual value of $L_{n,\mathrm{eff}}$ under these conditions, because the photocurrent variation produced by the Gaussian profile of the laser beam is significant for such small diffusion lengths. Four other devices yielded $L_{n,\mathrm{eff}}$ values under illumination of 4, 5, 6, and >7 μm, with the latter value limited by the contact-to-contact spacing in the device under study. The observed variation of $L_{n,\mathrm{eff}}$ is not surprising based on the proposed surface passivation mechanism. The highest measured value of 10.5 μm can thus be taken as a lower bound on the true bulk minority-carrier diffusion length of such wires. Measurements made at both forward and reverse bias, as well as zero-bias photovoltaic collection conditions, confirmed that the measured effective minority-carrier diffusion lengths were independent of bias, and thus rule out significant contributions from drift current to the $L_{n,\mathrm{eff}}$ measurements.

The bulk minority-carrier electron diffusion length is 2×10^{1} μm for p-Si that contains the thermodynamic equilibrium concentration (10^{17} atoms/cm^3) of Cu in Si at 1000 °C.[8] Hence, the $L_{n,\mathrm{eff}}$ measured for these Cu-catalyzed Si wires may still be limited by surface recombination and/or by the presence of other impurities in the bulk of the Si wires.

Bounds of $S\leq9\times10^{2}$ cm s^{-1} under broad-area illumination and $S\geq3\times10^{5}$ cm s^{-1} in the dark can be estimated from the measured values of $L_{n,\mathrm{eff}}$ for the best-performing device, assuming a bulk diffusion length of 2×10^{1} μm (see supporting information).[5,15] From the value of S measured in the dark, the Si–SiO_2 interface trap density can be estimated to exceed 3×10^{13} cm^{-2}, assuming reasonable values of the thermal velocity ($\nu_{\mathrm{th}}=10^{7}$ cm s^{-1}) and of the trap capture cross section ($\sigma=10^{-15}$ cm^2) [$D_{\mathrm{it}}=1/(S\bullet\sigma\bullet\nu_{\mathrm{th}})$]. This is a large interface trap density, but is comparable with previous results[5] and is much smaller than the surface density of Si atoms. Achievement of $L_{n,\mathrm{eff}}=10.5$ μm in Si microwires grown from a low-cost Si precursor is a significant result for Si wire array photovoltaics. Semiconductor device transport models suggest that wire array cells with a Si wire diameter of 3.0 μm, a wire length of 25 μm, and a 10^{18} cm^{-3} base doping concentration should be able to produce air mass 1.5, 1 sun, efficiencies of $\eta=14.5\%$.[16]

The authors thank BP, the Department of Energy Office of Basic Energy Sciences, and the Caltech Center for Sustainable Energy Research for support, as well as the Kavli Nanoscience Institute at Caltech, the Molecular Materials Research Center at Caltech, and the Center for the Science of Materials and Engineering (NSF MRSEC: DMR 0520565) for use of facilities, and thank Emily Warren, Josh Spurgeon, Brendan Kayes, and Michael Filler for their contributions.

[1] B. M. Kayes, M. A. Filler, M. C. Putnam, M. D. Kelzenberg, N. S. Lewis, and H. A. Atwater, Appl. Phys. Lett. **91**, 103110 (2007).
[2] B. M. Kayes, H. A. Atwater, and N. S. Lewis, J. Appl. Phys. **97**, 114302 (2005).
[3] M. D. Kelzenberg, D. B. Turner-Evans, B. M. Kayes, M. A. Filler, M. C. Putnam, N. S. Lewis, and H. A. Atwater, Nano Lett. **8**, 710 (2008).
[4] K. E. Plass, M. A. Filler, J. M. Spurgeon, B. M. Kayes, S. Maldonado, H. A. Atwater, and N. S. Lewis, Adv. Mater. (Weinheim, Ger.) **21**, 325 (2009).
[5] J. E. Allen, E. R. Hemesath, D. E. Perea, J. L. Lensch-Falk, Z. Y. Li, F. Yin, M. H. Gass, P. Wang, A. L. Bleloch, R. E. Palmer, and L. J. Lauhon, Nat. Nanotechnol. **3**, 168 (2008).
[6] M. C. Putnam, M. A. Filler, B. M. Kayes, M. D. Kelzenberg, Y. B. Guan, N. S. Lewis, J. M. Eiler, and H. A. Atwater, Nano Lett. **8**, 3109 (2008).
[7] W. M. Bullis, Solid-State Electron. **9**, 143 (1966).
[8] R. Sachdeva, A. A. Istratov, and E. R. Weber, Appl. Phys. Lett. **79**, 2937 (2001).
[9] See EPAPS supplementary material at http://dx.doi.org/10.1063/1.3247969 for further information on device fabrication, characterization, and analysis.
[10] E. J. Charlson and J. C. Lien, J. Appl. Phys. **46**, 3982 (1975).
[11] A. Many, Y. Goldstein, and N. B. Grover, *Semiconductor Surfaces* (Interscience, New York, 1965), p. 408.
[12] K. I. Seo, S. Sharma, A. A. Yasseri, D. R. Stewart, and T. I. Kamins, Electrochem. Solid-State Lett. **9**, G69 (2006).
[13] D. K. Schroder, *Semiconductor Material and Device Characterization*, 3rd ed. (Wiley, New York, 2006), p. 319.
[14] T. Hanrath and B. A. Korgel, J. Phys. Chem. B **109**, 5518 (2005).
[15] F. Daiminger, A. Schmidt, F. Faller, and A. Forchel, Proc. SPIE **2139**, 213 (1994).
[16] M. D. Kelzenberg, M. C. Putnam, D. B. Turner-Evans, N. S. Lewis, and H. A. Atwater, Proceedings of the 34th IEEE PVSC, 2009 (unpublished).